International Journal of Academic Research and Development
ISSN: 2455-4197
Impact Factor: RJIF 5.22
www.academicsjournal.com
Volume 2; Issue 6; November 2017; Page No. 653-662

FT-IR and FT-Raman spectral investigation, UV, NMR and DFT computations of 2, 3-dichloro-5-trifluoromethyl pyridine

[1] R Sangeetha, [2] Dr. S Seshadri, [3] Rasheed MP

[1] Research Scholar, PG and Research Department of Physics, Urumudhanalakshmi College, Trichy, Tamil Nadu, India
[2] Associate Professor and Head, PG and Research Department of Physics, Urumudhanalakshmi College, Trichy, Tamil Nadu, India
[3] Research Scholar, PG and Research Department of Physics, Urumudhanalakshmi College, Trichy, Tamil Nadu, India

Abstract
The solid phase FT-IR and FT-Raman spectra of 2, 3-Dichloro-5-Trifluoromethyl pyridine (2, 3-DC5TFMP) have been recorded in the regions 4000-400cm^{-1} and 3500-100cm^{-1}, respectively. The optimized geometric parameters, normal mode frequencies and corresponding vibrational assignments of the present sample are theoretically examined by means of B3LYP 6-311G ++ basis set. Besides, reliable vibrational assignments made on the basis of potential energy distribution. A close agreement was achieved between the observed and calculated frequencies by refinement of the scale factors. HOMO and LUMO analysis shows that charge transfer happens within the molecule. Mullikan investigation and the first order molecular hyperpolarizability of the compound were estimated. The UV-Vis spectrum and ^{1}H and ^{13}C NMR chemical shifts of the molecule were studied. Furthermore, Thermodynamic properties, NLO and MESP were likewise assessed and interpreted. Comparison of simulated spectra with the experimental spectra gives significant information about the ability of the computational technique to portray the vibrational modes.

Keywords: 2, 3-DC5T5MP, DFT, TD-DFT, HOMO, LUMO

1. Introduction
Vibrational spectra of substituted pyridine acquired big interest within the spectroscopic perspective of their obvious importance to biological systems and industrial significance. Literature survey reveals that substituted pyridine derivatives find applications in numerous fields such as paints, dyes, rubber products, adhesives, non-linear optical materials, photochemical and agricultural products. [1-10] A large amount of intermolecular association is possible in pyridine ring system due to its polarity. Detailed knowledge on the structures and spectral behaviour of pyridine derivatives is a necessary prerequisite for understanding, its chemical and biological properties. Herein, we describe our outcomes on various analyses of 2, 3-DC5TFMP through spectral measurements.

2. Materials and Methods
The fine sample of 2, 3-DC5TFMP was obtained from Sigma Aldrich, UK, and used as such for the spectral measurements. The room temperature FTIR spectrum of the compound was measured in the 4000–400cm^{-1} region at a resolution of ±1 cm^{-1}, using a BRUKER IFS-66V vacuum Fourier transform spectrometer equipped with a Mercury Cadmium Telluride (MCT) detector, a KBr beam splitter and globar source. The FT-Raman spectrum of 2, 3-DC5TFMP was recorded on a BRUKER IFS–66V model interferometer equipped with an FRA–106 FT-Raman accessory. The spectrum was recorded in the 3500–50 cm^{-1}. Stokes region using the 1064 nm line of an Nd: YAG laser for the excitation operating at 200 mW powers. The reported wave numbers are expected to be accurate to within ±1 cm^{-1}.

2.1 Computational Details
The molecular geometry optimization, energy and vibrational frequency calculations were done for 2, 3-DC5TFMP with the standard density functional triply parameter hybrid model DFT/ B3LYP. The 6-311 G ++ (d,p) basis set have been employed using the Gaussian 09 program [11]. Harmonic vibrational wavenumbers have been calculated using analytic second derivatives to confirm the convergence to minima on the potential energy surface and to evaluate the zero-point vibrational energy [12]. These force fields obtained in Cartesian coordinates and dipole derivatives with respect to atomic displacements were extracted from the archive section of the Gaussian 09 output and transformed to a suitably defined set of internal coordinates. The optimized geometrical parameters, IR intensity, Raman intensity, the atomic charges, dipole moment, reduced mass, force constant and other thermodynamic parameters were additionally figured. Scaling of the force field was performed according to the SQM procedure [13, 14] using selective scaling in the natural internal coordinate representation. [15, 16] The calculation of the potential energy distribution (PED) and the prediction of IR and Raman intensities were done on a PC with the MOLVIB program written by Sundius. [17, 18] For the plots of simulated IR and Raman spectra, pure Lorentzian band shapes were used with a bandwidth of 10 cm^{-1}. The symmetry of the molecule was also useful in making vibrational assignments. By combining the results of the Gauss view program [19] with symmetry considerations, vibrational frequency assignments

were made with a high degree of confidence. The defined local symmetry coordinates form complete set and matches quite well with the motions observed using the Gauss view program. ^{1}H and ^{13}C NMR chemical shifts were calculated with GIAO [20, 21] approach by applying B3LYP method. [22, 23]

2.2 Prediction of Raman Intensities

The Raman activities (Si) calculated with the GAUSSIAN 09 program and adjusted during the scaling procedure with MOLVIB were subsequently converted to relative Raman intensities (Ii) using the following equation (1) derived from the basic theory of Raman scattering. [24-26]

$$I_i = \frac{f(\nu_o - \nu_i)^4 S_i}{\nu_i\left[1 - \exp\left(\frac{-hc\nu_i}{kT}\right)\right]} \quad (1)$$

where ν_0 is the exciting frequency (in cm^{-1} units); ν_i i is the vibrational wave number of the of the ith normal mode, h, c and k are fundamental constants and f is a suitably chosen common normalization factor for all peaks intensities. Raman activities and calculated Raman intensities are reported in Table. 2.

3. Results and Discussion

3.1 Molecular geometry

The optimized most stable structure of title molecule is obtained from Gaussian 09W and Gaussview05 programs are shown in Fig.1. The comparative IR and Raman spectra of experimental and calculated frequencies are given in the Fig.2 and Fig.3.

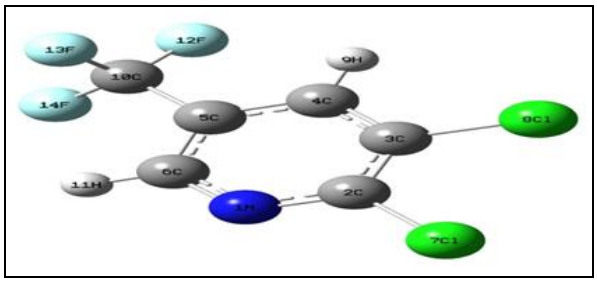

Fig 1: Molecular structure of 2, 3-DC5TFMP along with numbering of atoms

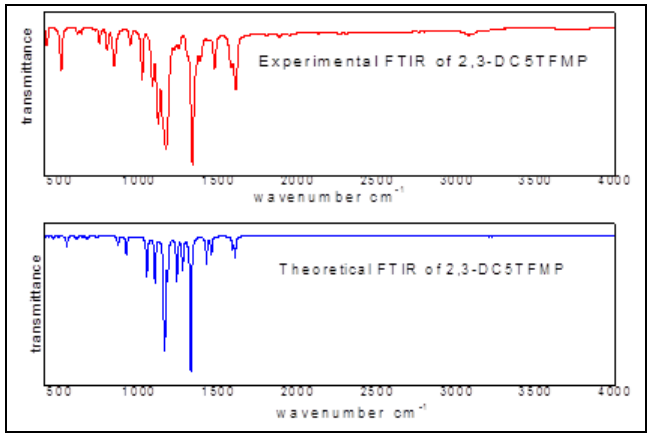

Fig 2: Comparison of Theoretical and experimental FTIR spectrum of 2, 3-DC5TFMP

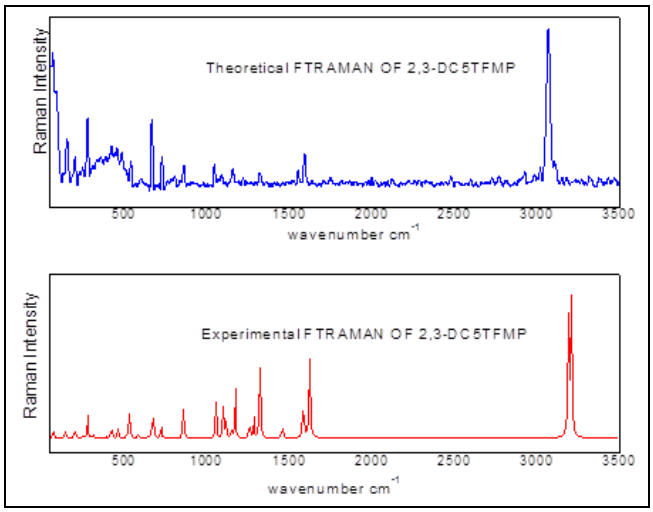

Fig 3: Comparison of Theoretical and experimental FT-Raman spectrum of 2, 3-DC5TFMP

The geometry of a molecule can be characterised by analysing the bond length and bond angle and torsional angle. Using B3LYP 6-311++G(d,p) basis set, bond length and bond angle and torsional values are given in Table.1.The calculated geometric parameters represent a good approximation and they are the bases for calculation of other parameters like vibrational frequency.

Table 1: Optimized geometrical parameters of 2, 3-DC5TFMP obtained by B3LYP/6-311++G (d, p) density functional calculations

Bond length	Angstorm (Å)	Bond angle	Degree	Torsional angle	Degree
C4-H9	1.0822	C3-C4-C5	118.95	H9-C4-C5-C10	2.74
C6-H11	1.0836	H9-C4-C5	121.1	H11-C6-N1-C2	-179.66
N1-C2	1.3174	H11-C6-N1	116.48	C2-N1-C6-C5	-0.09
N1-C6	1.3333	C2-N1-C6	119.26	N1-C6-C5-C4	0.07
C3-C4	1.3875	N1-C6-C5	122.31	C3-C4-C5-C6	-0.13
C5-C4	1.3932	C6-C5-C4	118.65	F12-C10-C5-C4	-35.08
C6-C5	1.3918	F12-C10-F14	107.57	F14-C5-F13-C10	53.56
F12-C10	1.3510	F14-C10-F13	106.97	F13-C5-F12-C10	54.14
F14-C10	1.3480	F13-C10-F12	106.74	Cl7-C3-N1-C2	0.1
F13-C10	1.3546	C10-C5-C6	121.05	Cl8-C4-C2-C3	0.11
C10-C5	1.5047	Cl8-C3-C2	122.5	C10-C4-C6-C5	2.02
Cl8-C3	1.7388	Cl7-C2-N1	116.57		
Cl7-C2	1.7436				

3.2. Vibrational Assignment

The theoretical investigations of 2, 3-Dichloro-5-Trifluoromethyl Pyridine were performed utilizing DFT B3LYP with 6-3-11++G (d, p) basis set. The calculated vibrational wavenumbers, measured infrared, Raman band positions and their vibrational assignments were exhibited in Table.2.

Table 2: Observed and B3LYP/6-311++G (d,p) level calculated vibrational frequencies (in cm^{-1}) of 2,3-DC5TFMP

S. No	symmetry species	Observed frequency		Calculated frequency (cm^{-1})with B3LYP/6-311++G(d,p) force field				Characterisation of normal modes with PED%
		IR (cm^{-1})	Raman (cm^{-1})	Unscaled (cm^{-1})	Scaled (cm^{-1})	IR intensity	Raman activity Si	
1	A"	-	-	17.7694	0.1	0.0906	0.8863	tCCCF(48), gCCCC(16)
2	A"	-	67.05	72.9033	0.2	0.5695	2.0963	tCCCH(58)
3	A'	-	-	140.2348	106.60.	1.3034	1.2272	gCC(46),tring(27),tCF3(25)
4	A"	-	153.04	145.2169	150.1	1.5429	0.4474	bCCl(46),bCC(28), bCCF(13)
5	A'	-	245.47	200.9594	182.0	0.0649	2.2116	bCCl(51),bCC(17),bCCF(12),]bNCl(10)
6	A'	-	-	246.9722	247.12	0.3200	0.4959	tCF3(72), bCCF(20)
7	A"	-	277.44	277.7407	277.1	0.4397	5.9034	CC(34),bring(34),CCl(11),bCCF(10)
8	A'	-	-	313.2489	312.9	0.2854	1.0986	bCCF(48),bCCl(25)
9	A'	-	393.58	393.5881	399.2	3.3541	0.3482	tring(50),bCCF(30), tCF3(14)
10	A"	-	422.52	424.4811	426.0	6.1476	2.9183	CCl(33),bCCl(27),bring(22)
11	A'	454.69	-	460.2438	453.1	0.7942	2.0121	bCCF(37),tCF3(18), bCC(15),bCCl(13)
12	A'	-	485.61	464.0204	483.7	0.7932	0.2935	tring(69),tCF3(20), gCH(10)
13	A"	540.77	-	519.7629	525.6	0.4047	0.7852	tCF3(48),tring(34),gCC(13)
14	A'	588.42	-	533.3690	540.9	40.4125	6.1956	CCl(45),bring(21),CC(15),
15	A"	641.28	-	582.2285	601.3	5.4560	0.8547	tCF3(30),CF(28),bCCF(17)
16	A"	666.46	-	641.9104	640.1	1.2925	0.4370	tring (68),tCF3(11)
17	A'	-	728.01	672.9465	669.2	5.5969	7.6009	bring(52),CCl(18),CC(18),
18	A"	732.96	-	721.6174	729.1	6.5444	3.5903	CF(38),bCCF(30), bring(16),
19	A'	-	-	741.2873	734.9	7.9630	0.1713	tCF3(45),tring (27),gCC(17),
20	A"	-	862.12	860.3486	862.9	28.1389	7.3176	bring(34),CCl(32), CC(16),CF(15)
21	A'	915.83	-	930.6520	916.0	28.3801	0.2838	gCH(48),tCF3(25), tring(14)
22	A'	-	-	957.7490	948.0	3.0941	0.0593	gCH(90)
23	A"	-	1046.98	1052.6120	1043.2	130.2166	9.6347	bring (59), CCl(20), CC(10)
24	A'	1090.18	-	1100.0603	1095.5	105.5062	8.1401	CC(35),CF(25),bCCF(13), bCH(12)
25	A'	-	1158.19	1117.3306	1154.2	280.1537	4.2823	CF(45),tCF3(27),bCCF(15)
26	A'	1159.56	-	1147.2688	1160.3	176.0403	1.7950	CF(47),tCF3(23),bCCF(12)
27	A'	-	-	1171.1908	1172.1	117.5541	13.7530	CCl(29),CC(29),bCH(20), CN(15)
28	A'	1224.60	-	1256.2558	1234.7	111.4984	5.0952	CC(46),CN(26),bCH(14)
29	A'	-	-	1283.6651	1277.7	14.8090	5.5478	CC(37),CN(33)
30	A'	-	1320.06	1323.4327	1322.2	381.3812	20.1480	CC(48),CF(11),bCH(11), bCCF(11)
31	A'	-	-	1409.9876	1415.2	68.9171	0.3380	CN(30),CH(28),CC(25)
32	A'	1433.55	-	1457.2113	1447.6	34.9963	4.2841	CC(27),bCH(25),CN(18), bNCH(10)
33	A'	1596.00	1593.29	1583.4053	1590.0	12.9139	13.3037	CC(54),CN(11)
34	A'	-	-	1623.7484	1602.8	70.7487	44.5615	CC(44), CN(24),bCH(18)
35	A'	3068.39	3074.49	3191.6243	3296.4	1.9657	97.5920	CH(99)
36	A'	-	3315.91	3210.8593	3315.9	1.7498	64.9375	CH(99)

(υ) stretching (b)bending; (g) scissoring and wagging ; (t) torsion; PED values are greater than 10% are given

3.2.1 C-H Stretching Vibrations

The hetero-aromatic compounds shows the presence of C-H stretching vibrations in the region 3100-3000 cm^{-1} which is the characteristic region for the ready identification of the C-H stretching vibration [27]. They are not appreciably affected by nature of substituent. In our title compound, the CH stretching modes of 2,3-DC5TFMP have been assigned at 3068.39 cm^{-1} in IR spectrum and C-H stretching mode in Raman spectrum is observed at 3074.49 and 3315.91 cm^{-1}. It's theoretically computed values for C-H stretching vibrations are found to be 3191.62 and 3210.85 cm^{-1} respectively. These stretching vibrations are scaled to 3296.4 and 3315.9cm^{-1} with a maximum 99% PED contribution.

The C-H in plane and out-of-plane bendings [28] were generally lie in the region 1300-1000cm^{-1} and 900-650cm^{-1} respectively. In accordance with the literature, in the present study, the bands observed at 1090, 224, 1433 cm^{-1} and 915.83 in FT-IR spectrum and 1320cm^{-1} and 485.61 cm^{-1} in FT-Raman spectrum were assigned to C-H –in-plane and out-of-plane bending vibrations respectively.

In this work, the C-H out-of-plane bending vibrations occur at 1009 and 915.83 cm^{-1} in IR spectrum and 485.61 in Raman spectrum. Here we have theoretically calculated values such as 1100.0603, 930.6520 in FT-IR spectrum and 464.02cm^{-1} which shows that the predicted values are coinciding very well with the observed frequencies.

When there is in-plane interaction above 1200 cm^{-1}, a carbon and its hydrogen usually move in opposite direction [29] Accordingly for our title compound 2,3-DC5TFMP, the C-H in-plane bending vibrations occur at 1224.60, and 1433.55 cm^{-1} respectively in IR spectrum and 1320.06 in FT Raman spectrum respectively.

3.2.2 C-C Vibrations

Generally the C-C stretching vibrations in aromatic compounds form the band in the region of 1430-1650 cm^{-1} [30].

The FTIR and Raman peaks observed at 1596.00, 1433.55, 1224.60 and 1090.18 in FTIR and 1593.29, 1320.06 and 1046.98cm^{-1} in FT-Raman are assigned to C-C stretching vibrations respectively. This shows good agreement with the experiment results.

3.2.3 C-N Vibrations

The identification of C-N vibrations is a very difficult task since mixing of several bands is possible in this region. The C-N stretching vibrations are always mixed with other bands and normally occur in the region 1266–1382 cm^{-1}. [31, 32]However with the help of force field calculations, the C-N stretching vibrations are identified and assigned in this work. The FTIR bands appearing at 1224.60, 1433.55 and 1596cm^{-1} respectively. The FT Raman band appearing at 1593cm^{-1} for 2, 3-DC5TFMP. The in-plane and out-of-plane bending vibrations assigned for 2,3-DC5TFMP are also presented in Table.2.Corresponding bands are theoretically calculated at 1256.25,1457.24 and 1593cm^{-1}.Theoretical and Experimental values are found to be in good agreement.

3.2.4 C-Cl Vibrations

The presence of halogen on alkyl substituted aromatic ring can be detected indirectly from its electronic impact on the in plane CH bending vibrations [33]. The strong peak in FTIR and FTRaman at 1000 cm^{-1} due to CH in plane bending confirms the presence of chlorine atom in our title compound. The C-Cl stretching vibrations give generally strong bands in the region 730-580cm^{-1}.Compounds with more than one chlorine atom exhibit bands due to asymmetric and symmetric modes [34-38]. The peaks at 588.42cm^{-1} in FTIR and 422.52, 728.01 and 862.12cm^{-1} in FT Raman is due to C-Cl stretching vibrations. The peak at 454.69 cm^{-1} in FTIR and 422.52 and 245.47cm^{-1} in FT Raman is due to C-Cl symmetric in plane bending vibration.

3.2.5 CF3 Vibrations

The CF3 group wavenumbers of the title molecule make a significant contribution to vibrational spectra. The title molecule 2, 3-DC5TFMP under consideration possesses one CF3 group. The bands observed at 1159.56, 915.83 641.28 and 540.77cm^{-1} in FT-IR and 1158.19 and 485.61 cm^{-1} in FT-Raman is in good agreement with the computed values by B3LYP at 1147.26,930.65, 582.22and 519.76 and 1099 cm^{-1} respectively.

The C–F deformation vibrations usually occur in the regions 640–580cm^{-1} and 590–490cm^{-1}.[39] The experimental peaks at 641.28 and 540.77cm^{-1} in FT-IR and 485 in FT-Raman spectra of the title compound confirm the presence of out-of-plane and in-plane bending vibrations of CF3. The calculated values by B3LYP methods at 582.22, 519.76 and 464.02 is in good agreement with experimental as well as the literature data.

CF3 rocking mode appears in the ranges of 450–350cm^{-1} and 350–260 cm^{-1} [39]. The peak appears at 393cm^{-1} is assigned to CF3 rocking mode. This is supported by the presence of bands at 393.58 cm-1 in FT-Raman spectra.

3.2.6 Ring Vibrations

Usually an in-plane deformation vibration is at higher frequencies than the out of plane vibration.In the present study, the bands observed at 737 cm^{-1} and 674 cm^{-1} in IR respectively attributed to ring in-plane bending modes. The ring out- of- plane bending mode frequencies are observed at 461 cm^{-1} in IR and 623 cm^{-1} in Raman spectra as shown in Table.2.

3.3 Thermodynamic Properties

The statistical thermo chemical investigation of 2, 3-DC5TFMP is done viewing the molecule to be at room temperature of 298.15K and one atmospheric pressure. The thermodynamic parameters, like rotational constant, zero point vibrational energy (ZPVE) of the molecule by DFT method (B3LYP). The variations in the zero point vibrational energy seem to be insignificant. The standard thermodynamic functions like heat capacity, entropy enthalpy, rotational constants and zero point vibrational energies of the compound were exhibited in Table.3 and Table.4. The correlation equations between these thermodynamic properties and temperatures were fitted by parabolic formula. All the thermodynamic data provide helpful information for the study on the title compound. From Table.3, it can be observed that the thermodynamic parameters are increasing with temperature ranging from 100K to1000K, due to the fact that the vibrational intensities of molecule with temperature [40].

Table 3: The Temperature dependence of Thermodynamic parameters of 2, 3-DC5TFMP

Temperature [T]	Energy[E] (KCal/Mol)	Heat capacity[Cv] (Cal/Mol-kelvin)	Entropy[s] (Cal/Mol-kelvin)
100	42.320	17.580	76.028
200	44.690	29.598	93.353
300	48.180	39.877	108.170
400	52.594	48.033	121.383
500	57.718	54.138	133.235
600	63.368	58.640	143.886
700	69.408	62.000	153.496
800	75.742	64.561	162.215
900	82.301	66.555	170.173
1000	89.039	68.136	177.480

Table 4: The Calculated Thermodynamical Parameters of 2, 3-DC5TFMP

Parameters	B3LYP/6311G(d,p)
Zero-point vibrational energy (Kcal/Mol)	46.57605
Rotational constants (GHz):	A 2.87460 B 0.45072 C 0.41850

The graph showing the correlation of heat capacity at constant pressure (Cp), entropy(S) and enthalpy change (ΔH0→T) with temperature is delineated in Fig.4, Fig.5 and Fig 6.

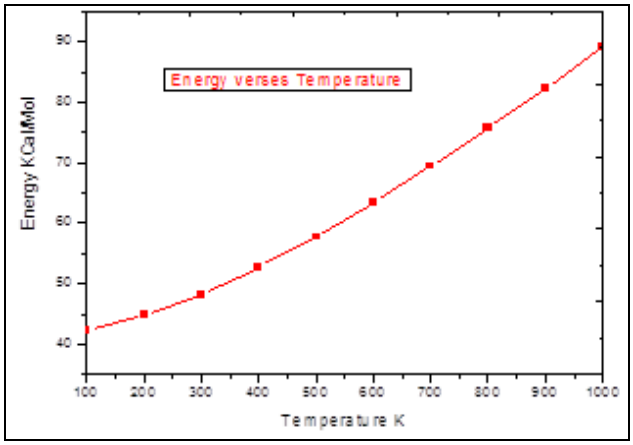

Fig 4: Temperature dependence of energy of 2, 3-DC5TFMP

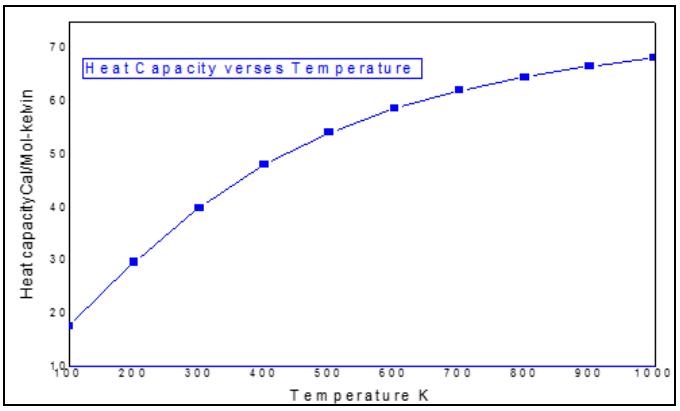

Fig 5: Temperature dependence of Heat capacity at Constant Volume of 2, 3-DC5TFMP

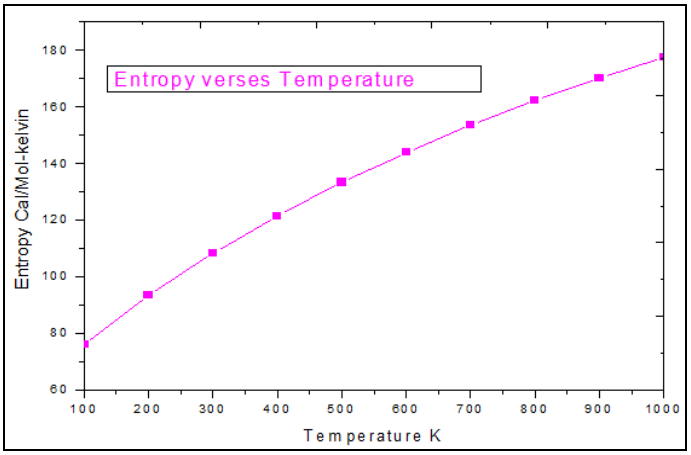

Fig 6: Temperature dependence of Entropy of 2, 3-DC5TFMP

3.4 Homo-Lumo analysis

The energies of two important molecular orbitals of 2, 3-DC5TFMP, the highest occupied molecular orbitals (HOMO) the lowest unoccupied (LUMO) were figured and portrayed in Fig.7. The energy gap between HOMO and LUMO is a basic parameter in deciding molecular electrical transport. Molecular orbitals (HOMO and LUMO) and their properties such as energy are very useful for physicists and chemists and are very important parameters for chemistry [41]. This is also used by the frontier electron density for predicting the most reactive position in л electron systems and also explains several types of reaction in conjugated system. This electron absorption corresponds to the transition from the ground to the first excited state and is mainly described by one electron excitation from the highest molecular orbital to the lowest unoccupied molecular orbital. Moreover, lower in the Homo and Lumo energy gap clarifies the eventual charge transfer [42] interactions taking place within the molecule. The Homo and Lumo energy calculated by B3LYP/6-311++G method is demonstrated as follows.

HOMO energy = -7.89457 eV
LUMO energy = 2.3029 eV
HOMO-LUMO energy gap = -5.5917eV

The atomic orbital compositions of the molecular orbitals are outlined in Fig.7. and the energy values of 2, 3-DC5TFMP were shown in Table.5. The energy gap between HOMO and LUMO demonstrates that our present sample have high band between the frontier molecular orbitals. In general, high HOMO-LUMO energy gap implies high kinetic stability and low chemical reactivity because it is energetically unfavourable to add electron to a high lying LUMO by extracting electrons from low lying HOMO.

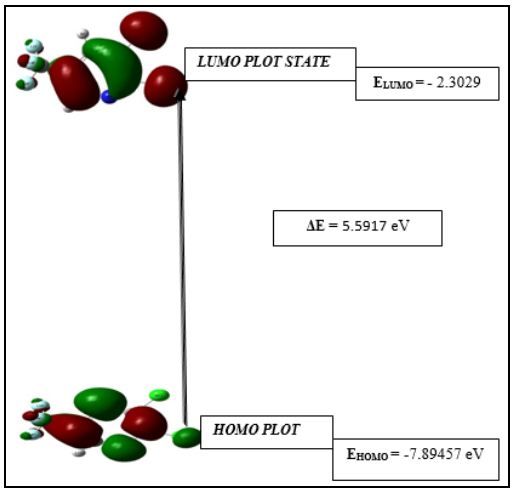

Fig 7: The atomic orbital compositions of the frontier molecular orbital (HOMO-LUMO) for 2, 3-DC5TFMP

Table 5: Energy values of 2, 3-DC5TFMP by B3LYP/6-311++G (d, p) method

Energies	Values
E_{HOMO} (eV)	-7.89457
E_{LUMO} (eV)	-0.2055
E_{HOMO} - E_{LUMO} gap (eV)	5.5917
Chemical hardness (η)	2.7958
Softness (S)	0.1788
Electronegativity (χ)	5.0987
Chemical potential (μ)	-5.0987
Electrophilicity index (ω)	4.6492

3.5. Mulliken Charges

The atomic charge in molecules is fundamental to chemistry. For instance, atomic charge has been used to describe the processes of electronegativity equalization and charge transfer in chemical reactions [43, 44], and to model the electrostatic potential outside molecular surfaces. Mulliken atomic charges calculated at the B3LYP/6-311++G (d, p) method is collected in Table.6. It is worthy to mention that N1, C3, C10, Cl7, Cl8,H9 and H11 atoms of 2,3-DC5TFMP exhibit positive charge, while C2,C4,C5 C6, F12, F13 and F14 atoms exhibit negative charges. The carbon atoms C2, C5 and C6 exhibit negative charges due to the presence of electron withdrawing property of chlorine and trifluoromethyl group. In addition, the Mulliken atomic charges, histogram of Mulliken charges was shown in Fig.9. and Fig.8.

Table 6: Atomic Charges for optimized geometry of 2, 3-DC5TFMP using DFT-B3LYP/6-311++G (d, p)

Atoms	Mullikken Atomic Charges
N1	0.158605
C2	-1.38242
C3	0.708706
C4	-0.34473
C5	-0.70296
C6	-0.11137
Cl7	0.516912
Cl8	0.572097
H9	0.245731
C10	0.386228
H11	0.237055
F12	-0.10342
F13	-0.06375
F14	-0.11669

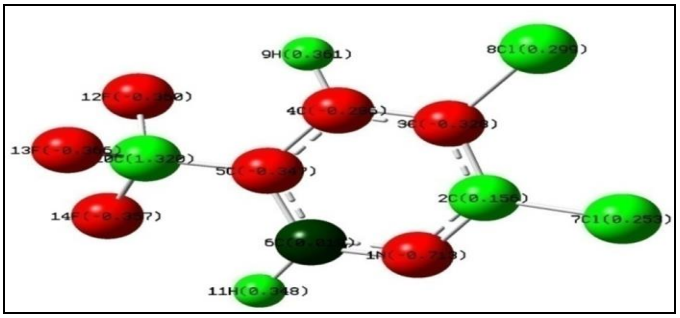

Fig 8: Mulliken atomic charges

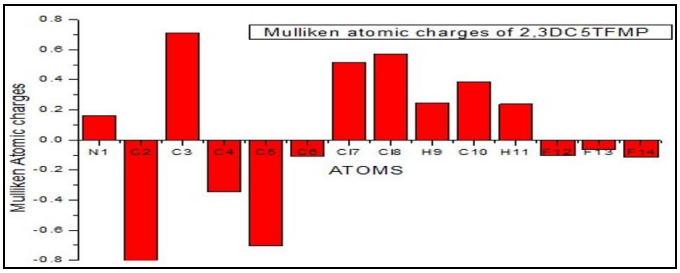

Fig 9: Histogram of calculated Mulliken charges of 2, 3-DC5TFMP

3.6 Analysis of molecular electrostatic potential (MESP)

Molecular Electrostatic potential map illustrate the charge distributions of molecules three dimensionally. These maps are very useful descriptor in understanding sites for electrophilic and nucleophilic reactions as well as hydrogen bonding interactions [45]. To predict reactive sites for the investigated molecule, MESP at the B3LYP /6-311++G (d,p) optimized geometry was calculated.

The different values of the electrostatic potential at the surface are represented by different colours. Potential increases in the order Red<orange<yellow<green<cyan<blue where blue (positive region) are related to nucleophilic reactivity [46]. The Electrostatic Potential from Total SCF Density mapped with esp is appeared in Fig.10(a) (Mesh view), Fig.10(b)(solid view) and Fig.11.Also, the contour map of positive and negative potential for 2, 3-DC5TFMP is appeared in Fig.12.

In the MESP map of the title compound, the maximum positive regions localized on the H9 atom in the ring. From this result, we can conclude that H atoms indicate the strongest attraction. In addition, the nitrogen atom and chlorine atom has slightly falls in the positive region and the fluorine atoms slightly falls in the negative region.

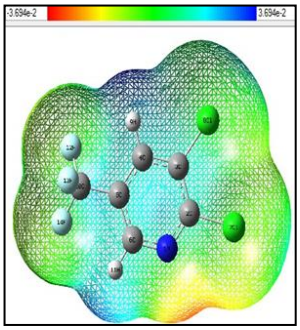

10(a) Mesh view

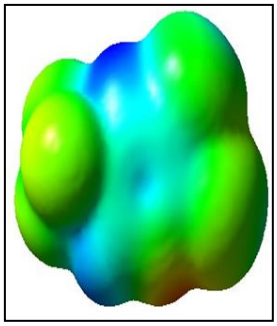

10(b) Solid view

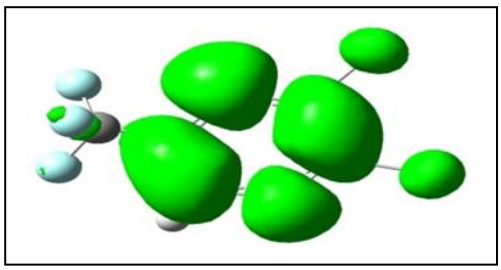

Fig 11: Electron density from total SCF density mapped with esp

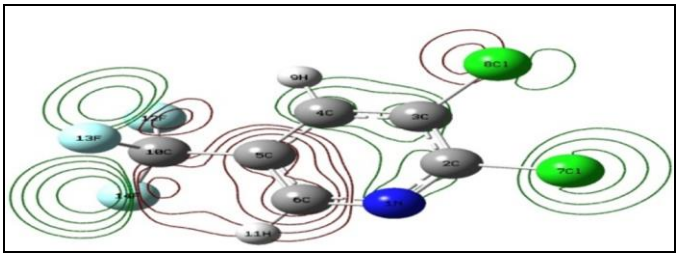

Fig 12: Contour Map of 2, 3-DC5TFMP

3.7 Hyperpolaraizability and NLO activity

Nonlinear optical (NLO) effects arise from the interactions of electromagnetic fields in diverse media to produce new fields altered in phase, frequency, amplitude or other propagation characteristics from the incident fields. [47]

In present study, the electronic dipole moment, molecular polarizabilility, anisotropy of polarizability and molecular first hyperpolarizability of present compound were investigated.The polarizability and hyperpolarizability tensors (αxx, αzy, αyy, αxz, αyz, αzz and βxxx, βxxy, βxyy, βyyy, βxxz, βxyz, βyyz, βxzz, βyzz and βzzz) can be obtained by a frequency job output file of Gaussian output are in atomic units (a.u.) (For α : 1a.u.= 0.1482× 10^{-24} esu; For β: 1a.u.=8.3×10^{-33} esu).The mean polarizability (α_{tot}), anisotropy of polarizability (Δα) and the average value of the first order hyperpolarizbilities (β_{tot}) can be calculated using the equations(2),(3) and(4).

$$A_{tot} = \alpha_{xx} + \alpha_{yy} + \alpha_{zz} / 3 \quad (2)$$

$$\frac{1}{\sqrt{2}} [(\alpha_{xx} - \alpha_{yy})^2 + (\alpha_{yy} - \alpha_{zz})^2 + (\alpha_{zz} - \alpha_{xx})^2 + 6\,\alpha^2_{xx}]^{1/2} \quad (3)$$

$$\beta = [(\beta_{xxx} + \beta_{xxy} + \beta_{xyy})^2 + (\beta_{yyy} + \beta_{xxz} + \beta_{yyz})^2 + (\beta_{xzz} + \beta_{yzz} + \beta_{zzz})^2]^{1/2} \quad (4)$$

In Table, the figured parameters portrayed below and electronic dipole moment μ_i (i=x,y,z) and the total dipole moment μ for the title compound are recorded. The total dipole moment can be calculated utilizing the below equation (5) [48].

$$\mu = (\mu x^2 + \mu y^2 + \mu z^2)^{1/2} \quad (5)$$

The components of polarizability and the first hyperpolarizability of the title compound can be seen in Table. 7. The total dipole moment and first order hyperpolarizability are 0.9080 Debye and 0.39917 ×10^{-30} esu respectively and are shown in Table.7.Total dipole moment of title molecule is approximately 1.0707 times greater than that of urea and first order hyperpolarizability is slightly greater than that of urea. So the result indicates that this compound may have nonlinearity of the molecule.

Table 7: The Calculated Electric dipole moment, Polarizability and First Hyperpolarizability of 2, 3-DC5TFMP

Dipole Moment μ		**Polarizability α**			**First order Hyperpolarizability β**		
Parameter	Value	Parameter	a.u	esu (× 10^{-24})	Parameter	a.u	esu (×10^{-33})
μ_x	-0.0440	α_{xx}	-87.982	13.038	β_{xxx}	-11.9184	1191.84
μ_y	0.9022	α_{xy}	3.1665	0.46927	β_{xxy}	1.163	10.0472
μ_z	-0.0923	α_{yy}	-80.7338	11.9647	β_{xyy}	-20.1923	1744.41
μ_{tot}	0.9080	α_{xz}	0.2184	0.032366	β_{yyy}	16.1542	1395.56
		α_{yz}	0.0141	0.0020896	β_{xxz}	-0.1424	1.2301
		α_{zz}	-81.7037	12.1085	β_{yyz}	1.249	0.60127
		α_{tot}	-83.4731	12.3707	β_{xzz}	-10.2315	10.7901
					β_{yzz}	1.1773	88.3899
					β_{zzz}	-0.896	10.1707
					β_{xyz}	0.0696	7.74054
					β	46.2055492	399.18
First order Hyperpolarizability β						0.39918×10^{-30} esu	

3.8 Donor-Acceptor interactions: Perturbation theory energy analysis

Table 8: Second order perturbation theory analysis of Fock matrix in NBO basis for 2, 3-DC5TFMP

Donor (i)	**Type**	**ED/e**	**Acceptor (i)**	**Type**	**ED/e**	**[a]E(2) (KJ mol^{-1})**	**[b]E(J)-E(i) (a.u.)**	**[c]F(I,j) (a.u.)**
N1-C2	σ	1.9841	N1-C6	σ*	0.0146	1.28	1.41	0.038
N1-C2	σ		C2-C3	σ*	0.05369	2.92	1.39	0.057
N1-C2	π	1.73218	C3-C4	π*	0.33895	11.62	0.33	0.056
N1-C6	σ	1.97687	C2-Cl7	σ*	0.05768	4.7	0.99	0.061
C2-C3	σ	1.98375	C3-C4	σ*	0.02672	3.21	1.31	0.058
C2-Cl7	σ	1.98687	N1-C6	σ*	0.0146	3.27	1.25	0.057
C2-Cl7	σ		C3-C4	σ*	0.05369	2.51	1.26	0.05
C3-C4	σ	1.97419	C2-C3	σ*	0.05369	3.9	1.26	0.063
C3-C4	σ		C2-Cl7	σ*	0.05768	4.32	0.89	0.056
C3-C4	σ		C4-C5	σ*	0.02232	3.16	1.3	0.057
C3-C4	σ	0.42741	N1-C2	σ*	0.03027	25.9	0.27	0.077

C3-C4	σ	0.32997	C5-C6	σ*	0.03	16.05	0.3	0.062
C3-Cl8	σ	1.98848	N1-C2	σ*	0.03027	2.7	1.27	0.052
C4-C5	σ	1.96715	C3-Cl8	σ*	0.03112	4.67	0.88	0.057
C4-C5	σ		C5-C6	σ*	0.03	4	1.28	0.064
C4-H9	σ	1.97603	C2-C3	σ*	0.05369	3.75	1.05	0.057
C5-C6	π		N1-C2	π*	0.42741	17.09	0.26	0.061
C5-C6	π		C3-C4	σ*	0.02672	26.23	0.28	0.076
C5-C6	π		C10-F13	σ*	0.10152	7	0.5	0.023
C5-C10	σ		C4-C5	σ*	0.02232	1.6	1.25	0.04
C6-H11	σ	1.98065	N1-C2	σ*	0.03027	4.48	1.07	0.062
C10-F12	σ	1.99508	C5-C6	π*	0.32997	1.23	1.57	0.039
C10-F13	π	1.99379	C5-C6	π*	0.32997	0.99	1.02	0.031
C10-F13	σ	1.99379	C4-C5	σ*	0.02232	1.37	1.57	0.042
N1	σ	1.88933	C2-C3	σ*	0.05369	10.2	0.86	0.085
N1	σ	1.88933	C5-C6	σ*	0.03	8.69	0.9	0.08
Cl7	π	1.96483	N1-C2	π*	0.42741	1	1.46	0.034
Cl7	π	1.96483	N1-C2	π*	0.42741	5.99	0.84	0.063
Cl7	LP(2)	1.96483	N1-C2	σ*	0.03027	17.07	0.29	0.069
Cl8	LP(3)	1.91422	C3-C4	π*	0.33895	13.68	0.31	0.063
F12	LP(2)	1.95444	C10-F13	σ*	0.10152	9.51	0.065	0.071
F12	LP(2)	1.95444	C10-F13	σ*	0.10152	10.92	0.66	0.076
F13	LP(2)	1.95279	C5-C10	σ*	0.05608	5.58	0.78	0.059
F13	LP(2)	1.95279	C10-F12	σ*	0.09247	10.21	0.65	0.073
F14	LP(3)	1.93774	C5-C10	σ*	0.05608	5.92	0.79	0.061
F14	LP(3)	1.93774	C10-F12	σ*	0.10152	11.23	0.63	0.077
F14	LP(3)	1.93774	C10-F13	σ*	0.10152	9.49	0.65	0.071

[a]$E^{(2)}$ means energy of hyper conjugative interaction (stabilization energy)
[b]Energy difference between donor and acceptor i and j NBO orbitals.
[c]F(i,j) is the Fock matrix element between i and j NBO orbitals

The NBO technique shows the bonding concepts like atomic charge, Lewis structure, bond type, bond order, and charge transfer and resonance possibility. Natural bond analysis is a useful tool for understanding delocalization of electron density from occupied Lewis-type (donor) NBOs to properly unoccupied non-Lewis (acceptor) NBOs within the molecule. The stabilisation of orbital interaction is proportional to the interaction is proportional to the energy difference between interacting orbitals. Therefore, the interaction having strongest stabilisation takes place between effective donors and effective acceptors. This bonding-antibonding interaction can be quantitatively described in terms of the NBO approach that is expressed by means of second order perturbation interaction energy $E^{(2)}$.[49]This stabilisation energy $E^{(2)}$ associated with i donor →j(acceptor) delocalisation is estimated from the second order perturbation approach as given below

$$E^{(2)} = q_i \frac{F^2(i,j))}{\epsilon_j - \epsilon_i} \qquad (6)$$

Where qi is the donor orbital occupancy, ϵ_i and ϵ_j are diagonal elements (orbital energies) and F (i,j) is the off-diagonal Fock matrix element.

Here for our present compound, several types of electronic interactions available between bonding, non-bonding and anti-bonding orbitals. In 2, 3-DC5TFMP, the highest stabilization about 26.23kJ mol^{-1} is observed at the interaction between π (C5-C6) → σ * (C3-C4). The π → π* type of transition was observed at the interaction between C5→ C6 and C1→ C2 is about 17.09 kJ mol^{-1}.

3.9 UV-Vis Spectral Analysis

Ultra violet spectral analysis of 2, 3–DC5TFMP has been investigated by TD-DFT /6-311++G (d, p) method. Calculations of molecular geometry show that the visible absorption maxima of this molecule correspond to the electronic transition from HOMO to LUMO. [50]The absorption bands occur at 261.15, 254.64 and 248.18 nm. The λmax is a function of substitution, the stronger the donor character substitution the more electrons pushed into the molecules, the larger the λmax. The electronic transition predicted for 2, 3–DC5TFMP by DFT method as shown in Fig.13. The theoretical electronic excitation energies, wavelength of the excitation and oscillator strengths were calculated and listed in Table. 9.

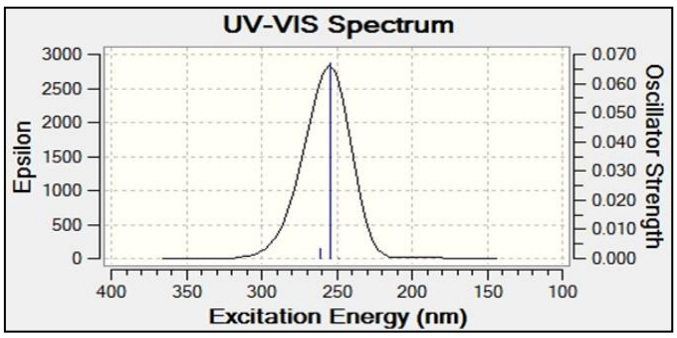

Fig 13: The UV-Visible Spectrum and excitation energy v/s oscillator strength of 2, 3–DC5TFMP

Table 9: Theoretical electronic absorption spectra values of 2, 3-DC5TFMP

Excited State	Energy (eV)	Wavelength λ (nm)	Oscillator strengths (f)
1	4.7476	261.15	0.0033
2	4.8691	254.64	0.0669
3	4.9957	248.18	0.0001

3.10 NMR Spectroscopy

Nuclear magnetic resonance (NMR) is a research technique that is used in many disciplines of scientific research. For reliable calculations of magnetic properties, accurate predictions of molecular geometries are essential. Firstly, full geometry optimization of 2, 3-DC5TFMP was performed at the gradient corrected density functional level of theory using the hybrid B3LYP method. [51] The experimental and theoretical ^{1}H and ^{13}C NMR chemical shift values for the title compound are listed in Table.10. The experimental ^{13}C and ^{1}H NMR spectra are shown in Fig.14.

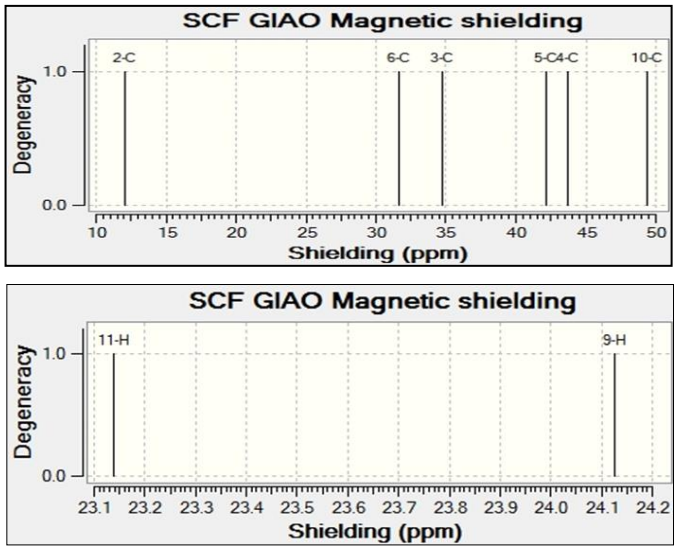

Fig 14: Theoretically calculated NMR spectrum of ^{13}C and ^{1}H for 2, 3-DC5TFMP

Table 10: Theoretically calculated NMR spectra of ^{1}H & ^{13}C for 2, 3-DC5TFMP

Atom	Chemical Shift(ppm)
C2	170.3763
C3	147.7313
C4	138.7653
C5	140.2786
C6	150.8283
C10	133.0972
H9	7.7564
H11	8.7441

The theoretical chemical shift values were calculated by Gauge Independant Atomic Orbital (GIAO) method using B3LYP /6-311++G (d, p) basis set. In general, highly shielded electrons appear downfield and vice versa. The high chemical shift values indicate the intermolecular hydrogen bonding in the studied molecule. C2 in pyridine ring appears at a higher chemical shift of 170 ppm due to neighbouring electronegative chlorine atom. The chemical shift value of C6 is the next higher due to the influence of electronegative nature of Nitrogen atom.

In our present investigation, the molecule under study contains two hydrogen atoms. The chemical shift of proton numbered H11 is highly towards the downfield when compare with other protons due to the influence of adjacent Nitrogen atom.

4. Conclusion

The equilibrium geometry and harmonic frequencies of 2, 3-DC5TFMP under investigation were determined and analyzed at DFT level employing the 6-311++G (d,p) basis set. The computed vibrational wavenumbers were assigned and compared with experimental FT-IR and FT-Raman spectra. The observed and stimulated spectra are in good agreement and show a good frequency fit of the title molecule. The molecular electrostatic potential surface investigation has additionally been utilized to clarify the property of 2,3-DC5TFMP.The present quantum chemical study may further play an important role in understanding of dynamics of the molecule. The HOMO-LUMO energy gap and other related molecular properties were discussed and reported. Theoretical UV-Vis spectrum was presented. ^{1}H and ^{13}C NMR chemical shift values were also studied. The values of dipole moment, linear polarizability and first order hyperpolarizability of the molecule were calculated. It has been found that the first-order hyperpolarizability is 1.0707 times greater than that of urea, which demonstrates that the molecule may have NLO property. In addition, NBO analyses were analysed and stabilisation values were given for our title compound.

5. References

1. Tomaru S, Matsumoto S, Kurihara T, Suzuki H, Oobara N, Kaino T. Appl. Phys. Lett. 1991; 58:2583-2585.
2. Kaneko C, Yamada S, Yokoe I, Hata N, Ubata Y, Tetrahedron Lett. 1966; 7:4729-4733.
3. Kaneko C, Yokoe I, Yamada S, Tetrahedron Lett. 1967; 8:775-778.
4. Hata N, Okutsu E, Tanaka I. Bull. Chem. Soc. J. 1968; 41:1769-1775.
5. Hata N, Ono I, Tuchiya T. Bull. Chem. Soc. Jpn. 1972; 45:2386-2391.
6. Ono I, Hata N. Bull. Chem. Soc. Jpn. 1972; 45:2951-2953.
7. Dopp D. in: Davidson (Ed.), Topics in Current Chemistry, vol. 55, Springer, Berlin, 1975.
8. Jose SP, Mohan S. Spectrochim. Acta. 2006; 64A:240-245.
9. Kirk-Othmer. Encyclopedia of Chemical Technology, fourth ed., 1997.
10. Pierrat P, Gros PC, Fort Y, J Comb. Chem. 2005; 7:879-886.
11. Mukherjee V, Singh NP, Yadav RA. J Mol. Struct. 2011; 988:24-34.
12. Pulay P, Fogarasi G, Pongor G, Boggs JE, Vargha A. J Am. Chem. Soc. 1983; 105:7037-7047.
13. Rauhut G, Pulay P, J Phys. Chem. 1995; 99:3093-3100.
14. Fogarasi G, Pulay P. in: JR Durig (Ed.), Vibrational Spectra and Structure, vol.14, Elsevier, Amsterdam. 1985, 125-219.
15. Fogarasi G, Zhou X, Taylor PW, Pulay P. J Am. Chem.

Soc. 1992; 114:8191-8201.
16. Sundius T, J. Mol. Struct. 1990; 218:321-326.
17. Sundius T. Vib. Spectrosc. 2002; 29:89-95.
18. Frisch A, Nielson AB, Holder AJ. Gaussview Users Manual, Gaussian Inc., Pittsburgh, PA, 2000.
19. Ditchfield R. J Chem. Phys. 1972; 56:5688-5691.
20. Wolinski K, James Hinton F, Pulay P. J Am. Chem. Soc. 1990; 112:8251-8260.
21. Azizi N, Rostami AA, Godarzian A. J Phys. Soc. Jpn. 2005; 74:1609-1620.
22. Rohlfing M, Leland C, Allen C, Ditchfield R. Chem. Phys. 1984; 87:9-15.
23. Kalsi PS. Spectroscopy of Organic Compounds, Sixth ed., New Age International (p) Limited Publishers, New Delhi, 2005.
24. Polavarapu PL, J Phys. Chem. 1990; 94:8106-8112.
25. Keresztury G, in: Chalmers JM, Griffiths PR. (Eds.), BT Raman Spectroscopy: Theory in Handbook of Vibrational Spectroscopy, John Wiley & Sons Ltd. 2002; 1:71-87.
26. Keresztury G, Holly S, Varga J, Besenyei G, Wang AY, Durig JR. Spectrochim. Acta Part A. 1993; 49:2007-2026.
27. Seshadri S, Sangeetha R, Rasheed MP, Padmavathy M. International Research Journal of Engineering and Technology (IRJET). 2016; 3(10).
28. Keresztury G. Raman Spectroscopy: Thorey, in: J.M. Chalmers, P.R. Griffths (Eds.), Handbook of Vibrational Spectroscopy, vol. 1, John Wiley & Son, New York, 2002.
29. Sangeetha JR, Seshadri S, Rasheed MP. International Journal of Advanced Engineering and Research Development. 2017; 4(8).
30. Krishna kumar V, Surumbarkuzhali N, Muthunatesan S, Spectrochim. Acta Part A. 2009; 71:1810-1813.
31. Shlyapochnikov VA, Kgaihin LS, Grikina OE, Bock CW, Vilkov LV. J Mol. Struct. 1994; 326:1-16.
32. Ataly Y, Avci D, BaSoglu A. Struct. Chem. 2008; 19:239-246.
33. Coates J. Interpretation of infrared spectra–apractical approach, in: R.A. Meyers (Ed.), Encyclopedia of Analytical Chemistry, John Wiley & Sons Ltd., Chichester. 2000, 10815-10837.
34. Higuichi SJ. Spectrochim. Acta A 1974; 30:463.
35. Wiffen DH. Spectrochim. Acta. 1955; 7:253.
36. Murto J, Spectrochim. Acta A. 1973; 29:1125.
37. Risgin JH. Fluorocarbons and Related Compounds – Fluoro Carbon Chemistry, Academic Press, New York. 1954; 2:449.
38. Lian CY, Krimm S. J Chem. Phys. 1956; 25:563.
39. Socrates G. Infrared and Raman characteristic Group Frequencies 3rd ed (John Wiley, Chic ester. 2001, 209.
40. Bevan J, Ott J. Boerio-Goates Chemical Thermodynamics: Principles and Applications, Academic Press, San Diego, 2000.
41. Fukui K, Yonezawa T, Shingu H. J Chem. Phys 1952; 20:722-725.
42. Muthu S. J Uma Maheswari, Spectrochimica Acta Part A: Molecular and Biomolecular Spectroscopy, Part A. 2012; 92:154-163.
43. Jug K, Maksic ZB. in: Z.B. Maksic (Ed.), Theoretical Model of Chemical Bonding, Part 3, Springer, Berlin. 1991, 233.
44. Fliszar S. Charge Distributions and Chemical Effects, Springer, New York, 1983.
45. Luque FJ, Lopez JM, Orozco M. Theor. Chem. Acc. 2000; 103:343-345.
46. Seshadri S, Sangeetha R, Rasheed MP, Padmavathy M. International Research Journal of Engineering and Technology (IRJET). 2016; 3(10).
47. Sun YX, Hao QL, Wei WX, Yu ZX, Lu LD, Wang X. *et al*. Theochem. 2009; 904:74-82.
48. Mekala R, Mathammal R, Sangeetha M, Theoretical Investigation of the Molecular Structure, Vibrational Spectra, NMR, UV, NBO Analysis, Homo and Lumo Analysis of 2-(1-Piperazinyl)Ethanol. J Theor Comput Sci. 2015; 2:3.
49. Arjunana V, Saravanan I, Mythili CV, Kalaivani M, Mohan S. Spectrochimica Acta Part A: Molecular and Biomolecular Spectroscopy, Spectrochimica Acta Part A. 2012; 92:1-15.
50. Seshadri S, Rasheed MP, Sangeetha R. Quantum Mechanical Study of the Structure and Spectroscopic (FTIR, FT-Raman, NMR and UV), First Order Hyperpolarizability and HOMO-LUMO Analysis of 2-[(Methylamino) Methyl] Pyridine, IOSR Journal of Applied Physics. 2015; 2(6):56-70.
51. Cavalli A, Salvatella X, Dobson CM, Vendruscolo M. Proc. Natl. Acad. Sci. USA, 2007; 104:9615-9620.